Geochemistry, Geophysics, Geosystems

RESEARCH ARTICLE
10.1029/2021GC009670

Key Points:

- Sixty-one repeating earthquake families were identified between 2003 and 2020 near the Raukumara Peninsula, northern Hikurangi subduction margin, New Zealand
- Family focal mechanisms are consistent with both intra- and inter-plate faulting
- The repeating earthquakes coincide with previously identified slow-slip events and locate around the down-dip edge and between main slow-slip patches

Supporting Information:

Supporting Information may be found in the online version of this article.

Correspondence to:

L. Hughes,
hughes.lauragrace@gmail.com

Citation:

Hughes, L., Chamberlain, C. J., Townend, J., & Thomas, A. M. (2021). A repeating earthquake catalog from 2003 to 2020 for the Raukumara Peninsula, northern Hikurangi subduction margin, New Zealand. *Geochemistry, Geophysics, Geosystems*, *22*, e2021GC009670. https://doi.org/10.1029/2021GC009670

Received 21 JAN 2021
Accepted 30 MAR 2021

A Repeating Earthquake Catalog From 2003 to 2020 for the Raukumara Peninsula, Northern Hikurangi Subduction Margin, New Zealand

Laura Hughes[1], Calum J. Chamberlain[1], John Townend[1], and Amanda M. Thomas[2]

[1]School of Geography, Environment and Earth Sciences, Victoria University of Wellington, Wellington, New Zealand, [2]Department of Earth Sciences, University of Oregon, Eugene, OR, USA

Abstract Repeating earthquakes provide a novel way of monitoring how stresses load faults between large earthquakes. To date, however, and despite the availability of long-duration, high-quality seismological datasets, little attention has been paid to tectonic repeating earthquakes in New Zealand. We develop a workflow and composite criterion for identifying repeating earthquakes in New Zealand, using data from the GeoNet permanent seismic network, and present New Zealand's first decadal-scale repeating earthquake catalog. For events to be identified as repeating in this study, two or more events must have a normalized cross-correlation of at least 0.95 at two or more seismic stations, when calculated for 75% of the earthquake coda. By applying our composite criterion to seismicity around the Raukumara Peninsula, northern Hikurangi subduction margin, we have identified 61 repeating earthquake families occurring between 2003 and 2020, consisting of 347 individual earthquakes. These families have a magnitude range of M_L 1.7–5.2 and recurrence intervals of <1 to ~7 yrs. Repeating earthquakes in 9 of the 11 regional groups identified in this study coincide spatiotemporally with previously identified slow-slip events and tremor. However, the responses shown to slow-slip are not consistent within families or within regional groups.

Plain Language Summary Repeating earthquakes are earthquakes that re-rupture the same fault patch thereby producing highly similar seismograms and occur sporadically and in some cases periodically through time. In this study, we developed a methodological workflow and a composite criterion for identifying repeating earthquakes in New Zealand, using data from the GeoNet permanent seismic network. The composite criterion is similar to that used in previous repeating earthquake studies at plate boundary zones elsewhere but is customized to the available data and earthquake sources of interest. We identified 61 repeating earthquake families, consisting of 347 individual earthquakes, which occurred between 2003 and 2020 around the Raukumara Peninsula, northeastern North Island. The location and timing of the repeating earthquake families coincide with those of previously identified slow-slip and tremor.

1. Introduction

Monitoring and interpreting how stresses load faults in the run-up to large earthquakes, and what impact this has on nucleation and rupture processes, remains a significant challenge in earthquake physics (e.g., Passelègue et al., 2020). Repeating earthquakes provide one means of monitoring these processes within the seismogenic portions of faults (Uchida, Matsuzawa, Hasegawa, et al., 2003). In New Zealand, little attention has been paid to repeating earthquakes, despite the availability of high-quality, long-duration seismological datasets. In this paper, we describe the construction and analysis of the first decadal-scale (17 yr) catalog of repeating earthquakes of tectonic origin in New Zealand.

1.1. Repeating Earthquakes

Repeating earthquakes are identified primarily on the basis of their highly similar waveforms, observed at multiple stations, which imply similar hypocenters and focal mechanisms (e.g., Chen, Bürgmann, & Nadeau, 2013; Li et al., 2018; Nadeau, Antolik, et al., 1994; Nadeau & Johnson, 1998; Naoi et al., 2015; Senobari & Funning, 2019; Uchida, Matsuzawa, Hasegawa, et al., 2003; Zhang et al., 2008). Due to their similarities,

it is hypothesized that repeating earthquakes represent the repeated rupture of the same strong asperity or fault patch (e.g., Nadeau & McEvilly, 1999; Uchida, Matsuzawa, Hasegawa, et al., 2003). Repeating earthquakes have been the subject of extensive research at several plate boundary zones, notably the Japan Trench (e.g., Hatakeyama et al., 2017; Uchida, Matsuzawa, Hasegawa, et al., 2003) and the San Andreas fault system (e.g., Abercrombie et al., 2020; Nadeau, Antolik, et al., 1994; Thomas et al., 2016; J. R. Williams et al., 2019), as well as China (e.g., Schaff & Richards, 2004), Taiwan (e.g., Chen et al., 2008), Costa Rica (e.g., Chaves et al., 2020; Yao et al., 2017), Greece (e.g., Mesimeri & Karakostas, 2018), and the Tonga–Kermadec Trench (e.g., Yu, 2013).

If, as hypothesized, repeating earthquakes represent repeated failure of the same fault patch, due to successive phases of loading and slip, then their magnitudes—or equivalently their stress-drops, assuming the same rupture area—and inter-event times will be interpretable in terms of stressing-rate (e.g., Nadeau, Antolik, et al., 1994). Furthermore, the interaction between repeating earthquakes within a family, between different families, and with nearby and distal seismic and aseismic phenomena may provide insights into fault properties (e.g., Marone et al., 1995) and changes in the surrounding stress field (e.g., Lui & Lapusta, 2016; Nadeau, Foxall, et al., 1995). The interaction between large earthquakes nearby and repeating earthquake families can also provide information about how stresses are loading the small asperities on which repeating earthquakes are assumed to be occurring (Chen, Bürgmann, & Nadeau, 2013; Chen, Bürgmann, Nadeau, Chen, et al., 2010; Wu et al., 2014). Repeating earthquakes have also been recorded during episodes of slow-slip (Kato et al., 2012; Shaddox & Schwartz, 2019) and have been used as a proxy to monitor aseismic creep prior to large earthquakes (e.g., Kato et al., 2012; Mavrommatis et al., 2015).

Fault slip-rates can be estimated from repeating earthquake observations using either the recurrence interval and seismic moments of the repeating earthquakes (e.g., Mavrommatis et al., 2015; Nomura et al., 2017) or the average seismic moment of the family (e.g., Nadeau & Johnson, 1998; Uchida, Matsuzawa, Hasegawa, et al., 2003). Slip-rates can then be determined by dividing the estimated slip by the repeating earthquake family duration. An extension of this allows variable slip-rates to be modeled to show changes in the amount and rate of slip on the fault patches where repeating earthquakes are occurring (Mavrommatis et al., 2015; Nadeau & Johnson, 1998; Nomura et al., 2017). Changes in slip-rate recorded by repeating earthquake families have been observed in the lead up to, and/or following, large earthquakes (Mavrommatis et al., 2015; Nomura et al., 2017). Hence, our work provides the first step to potentially monitoring changes in slip-rate *in situ* at seismogenic depths around the plate boundaries of New Zealand.

1.2. Tectonic Setting

The Hikurangi subduction margin accommodates convergence of the Australian and Pacific Plates and runs the length of the North Island of New Zealand (Clark et al., 2019), posing the largest seismic hazard for New Zealand (Clark et al., 2019). Due to the risk of great earthquakes ($M \geq 8$) occurring along this margin, extensive research has been undertaken to examine and quantify the associated hazard and risks (Clark et al., 2019, and references therein). Convergence rates vary from 32 mm/yr in the south, to 54 mm/yr in the north. Interface coupling also varies along the margin, with the interface locked to ~35 km depth in the south but only to ~10 km depth in the north (Wallace, 2020; Wallace, Reyners, et al., 2009).

The Raukumara Peninsula lies above the northern Hikurangi subduction margin in the northeast of New Zealand's North Island (Figure 1). Here, the Pacific Plate is subducting beneath the Australian Plate with convergence rates at the trench ranging from ~47 mm/yr at the southern extent of the Peninsula, to ~57 mm/yr to the north (Figure 1) (Wallace, Beavan, Bannister, et al., 2012). Beneath the eastern edge of the Raukumara Peninsula, the plate interface is inferred to lie at ~12–15 km and it progressively deepens to ~50 km beneath the western edge (C. A. Williams, et al., 2013). Upper plate faults in the North Island Dextral Fault Belt in the overriding Australian Plate accommodate much of the right-lateral strike-slip component of the Australia-Pacific relative plate motion (Figure 1) (Beanland, 1995; Nicol & Wallace, 2007; Wallace, Beavan, McCaffrey, et al., 2004). Reverse faults have been imaged offshore from the Raukumara Peninsula and accommodate part of the convergent component of relative plate motion (Barnes et al., 2010; Litchfield et al., 2020; Mountjoy & Barnes, 2011).

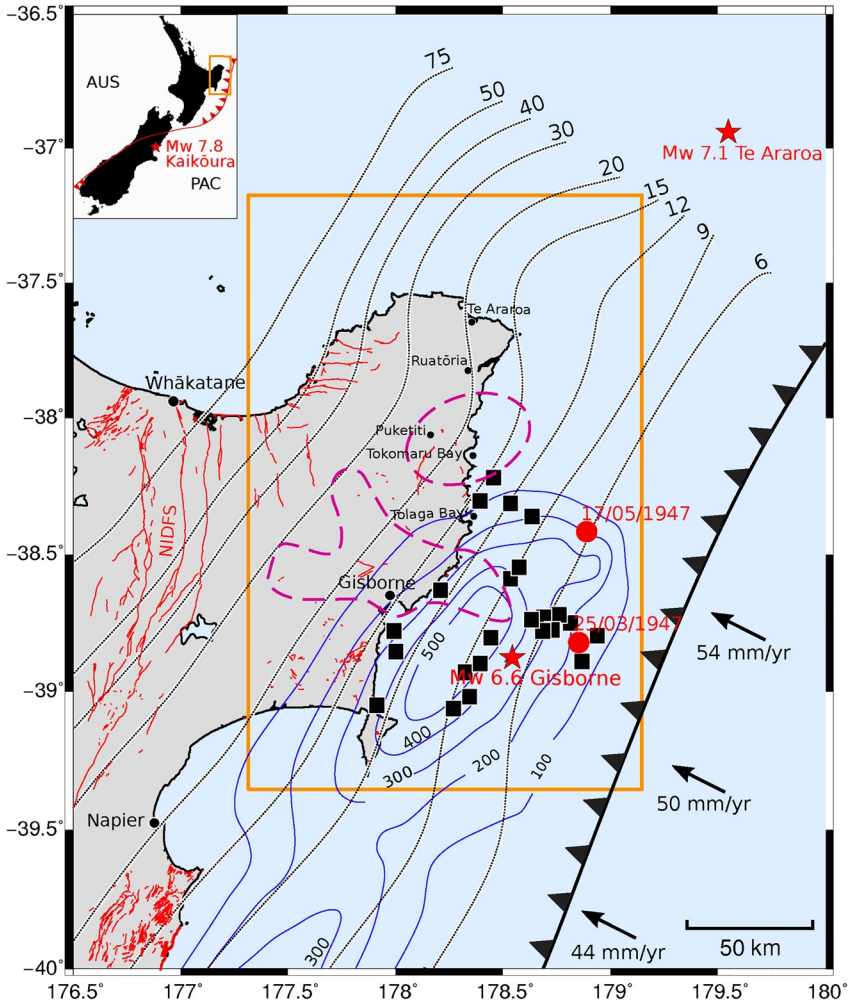

Figure 1. Seismic and aseismic phenomena recorded around the Raukumara Peninsula. Black arrows represent the convergence rates at the trench (Wallace, Beavan, Bannister, et al., 2012) and black dotted lines represent the depth (labeled in km) to the plate interface (C. A. Williams et al., 2013). Red stars mark the locations of the M_W 6.6 Gisborne earthquake of 2007 and the M_W 7.1 Te Araroa earthquake of 2016. Red circles represent the location of two tsunami-generating earthquakes that occurred in 1947 (Bell, Sutherland, et al., 2010). Filled black boxes mark the locations of burst-type repeating earthquakes between May 2014 and July 2015 that were reported by Shaddox and Schwartz (2019). Purple dashed contours demarcate locations of tremor between 2010 and 2015 identified by Todd and Schwartz (2016). Blue contours represent the cumulative slow slip, in mm, that occurred between 2002 and 2014, as described by Wallace (2020). The orange box in the main panel indicates the focus area of this study. Red lines represent active faults from the New Zealand Active Fault Database (Langridge et al., 2016), including the North Island Dextral Fault System (labelled as NIDFS). Inset: Map of New Zealand showing the study area in a larger context and the location of the M_W 7.8 Kaikōura earthquake. AUS represents the Australian Plate and PAC represents the Pacific Plate.

These tectonic components exhibit a wide range of transient seismic phenomena throughout the Raukumara Peninsula and surrounding region (Wallace, Reyners, et al., 2009), including moderate- to large-magnitude earthquakes ($M \leq 7.2$) (Francois-Holden et al., 2008; Koulali et al., 2017; Warren-Smith, Fry, Kaneko, et al., 2018), repeated episodes of shallow and deep slow-slip (e.g., Douglas et al., 2005; Wallace, 2020; Wallace & Beavan, 2010; Wallace, Beavan, Bannister, et al., 2012; Wallace, Hreinsdóttir, et al., 2018; Wallace, Webb, et al., 2016), tectonic tremor (Todd & Schwartz, 2016; Todd et al., 2018), triggered seismicity (Delahaye et al., 2009), and recently documented burst-type repeating earthquakes (Shaddox & Schwartz, 2019) (Figure 1). Several large earthquakes have occurred across the region in the last century. Of particular note are two M_W 7.2 tsunamigenic earthquakes that occurred in March and May of 1947 off the coast of Gisborne and Tokomaru Bay (Bell, Holden, et al., 2014; Doser & Webb, 2003), a normal-faulting intraslab M_W 6.6 event offshore from Gisborne in December 2007 (Francois-Holden et al., 2008), and the M_W 7.1 Te Araroa (TA)

earthquake of September 2016 (Koulali et al., 2017; Warren-Smith, Fry, Kaneko, et al., 2018). These larger events appear to often involve interactions with other seismic phenomena: for instance, the TA earthquake was preceeded by slow-slip events (SSEs) (Koulali et al., 2017; Warren-Smith, Fry, Kaneko, et al., 2018).

Repeated slow-slip is a common occurrence along the eastern edge of the Raukumara Peninsula (Wallace, 2020). At the northern end of the Hikurangi subduction margin, SSEs have typical recurrence intervals of 18–24 months (e.g., Douglas et al., 2005; Wallace & Beavan, 2010; Wallace, Webb, et al., 2016). The equivalent moment magnitudes of these SSEs are M_W6.3 to 7.2, and they typically occur at depths of less than 15 km (Koulali et al., 2017; Wallace & Beavan, 2010). SSEs along most of the Hikurangi subduction margin were triggered by the 2016 M_W7.8 Kaikōura earthquake in the weeks to months that followed (Wallace, Hreinsdóttir, et al., 2018).

SSEs have been observed simultaneously with both tremor (e.g., Todd & Schwartz, 2016; Todd et al., 2018) and distinctive microseismicity (Delahaye et al., 2009), at the northern Hikurangi subduction margin. Todd and Schwartz (2016) and Todd et al. (2018) concluded that the northern Hikurangi SSEs tend to be accompanied by tremor, which typically occurs down-dip of the geodetically determined slip patch, and typically occur toward the end of the SSE and afterward. Tremor has been most commonly observed during the larger-magnitude SSEs around the Gisborne area, but has also been documented during smaller SSEs further north in the vicinity of Tolaga Bay and Puketiti. However, tremor associated with offshore SSEs is often difficult to detect using New Zealand's entirely land-based national seismic network (Delahaye et al., 2009; Todd & Schwartz, 2016; Todd et al., 2018), complicating interpretation of its relationship to SSEs.

Recently, "burst-type" repeating earthquakes have been identified near the Raukumara Peninsula following the 2014 Gisborne SSE (Figure 1; Shaddox & Schwartz, 2019). These repeating earthquakes were inferred to occur on an upper-plate fracture network above a subducting seamount, and were only observed to be active for a short time period (approximately 7 weeks; Shaddox & Schwartz, 2019). We note that such "burst-type" repeating earthquakes were detected using less stringent waveform similarity criteria than employed in most other repeating earthquake studies referred to above (cf. Uchida & Bürgmann, 2019) and may not represent the repeated slip of exactly the same asperity. Other than the study by Shaddox and Schwartz (2019) of burst-type repeating earthquakes accompanying the 2014 Gisborne SSE, no long-duration analyses of tectonic repeating earthquakes have been undertaken around the Raukumara Peninsula. A 7-yr catalog, containing 1,398 repeating earthquake clusters, of two or more events, was identified by Wallace, Kaneko, et al. (2017) to the south of the Raukumara Peninsula (−40° – 41°S, 175.5° – 177.5°E). It is noted by Wallace, Kaneko, et al. (2017) that most of those clusters occurred in the aftershock zone of the January 20, 2014, M 6.2 Eketāhuna earthquake. These repeating earthquakes are not compared to the catalog identified here, as they occurred outside of the area of interest for this study.

1.3. Repeating Earthquake Identification Around the Raukumara Peninsula

In this paper, we describe the construction and interpretation of the first decadal-scale tectonic repeating earthquake catalog in New Zealand. We have focused our search for repeating earthquakes on the Raukumara Peninsula, due to the high levels of seismicity observed in the region and the large number of previously documented interactions between seismic and aseismic deformation phenomena occurring in the northern Hikurangi subduction margin (Wallace, 2020).

The first step in our analysis has been to develop and test a workflow and composite detection criterion for identifying repeating earthquakes in the New Zealand context using data from the GeoNet network. Waveform cross-correlation is the most commonly used method for identifying repeating earthquakes (Nadeau, Antolik, et al., 1994; Senobari & Funning, 2019; Uchida & Bürgmann, 2019). Cross-correlations are calculated for candidate pairs of earthquakes that are within a given hypocentral distance of one another, with the events being identified as repeating if they have a normalized cross-correlation exceeding some threshold (commonly 0.90–0.95) at multiple seismic stations (e.g., Nadeau, Foxall, et al., 1995; Nomura et al., 2017). While the majority of studies follow this general approach, each study has adapted components of the detection criteria to local conditions and requirements, including the length of the waveforms used to calculate the cross-correlation, the number of stations required, the filtering applied to the waveforms,

and the threshold imposed to cope with particular geometries and data quality (e.g., Bohnhoff et al., 2017; Nadeau & Johnson, 1998).

2. Methods

2.1. Dataset and Initial Clustering

We constructed our catalog of repeating earthquakes starting with the GeoNet seismicity catalog from January 1, 1987, to July 26, 2019 (as downloaded from the GeoNet International Federation of Digital Seismograph Networks (FDSN), service (https://www.geonet.org.nz/data/tools/FDSN) on July 26, 2019). We downloaded waveform data from the GeoNet FDSN service using ObsPy (Krischer et al., 2015) for all broadband and short-period stations and channels represented by the cataloged picks. We used only the picked stations, rather than, for example, all stations within a specified radius of the earthquake, to ensure that poor-quality (low signal-to-noise) waveforms were not included in the clustering. We note that this potentially introduces a bias related to varying picking protocols through time, but is preferably to introducing potentially lower-quality data to our correlations.

We first clustered the entire GeoNet catalog of 570,671 earthquakes throughout New Zealand based on inter-event separation and multi-station averaged inter-event cross-correlation. This initial clustering was conducted with a low cross-correlation threshold (0.75) and relatively large inter-event separation (30 km) to allow for location uncertainties. Note that throughout this paper the term "cross-correlation" refers to fully normalized cross-correlation.

In this initial step, cross-correlations were computed on the vertical channels of 2–15 Hz instrument-response-corrected bandpassed data resampled to 50 Hz beginning 2 s before the P-pick and of 6 s duration. Single-station correlations were allowed to shift by ±1.5 s to allow for pick uncertainty, and the maximum cross-correlations for each station were averaged to generate a mean inter-event cross-correlation. For each pair of events, we computed correlations only for stations picked by GeoNet for both events. Cross-correlations were only computed for pairs of events with hypocentral separations of less than 30 km to reduce computational demands. To cope with multiple possible groupings, we used a hierarchical clustering approach, as implemented in SciPy (Virtanen et al., 2020) and applied using EQcorrscan (Chamberlain et al., 2018) to assign earthquakes to clusters of potentially repeating events (herein termed "families").

The purpose of this initial clustering step was to reduce the size of the dataset and allow efficient testing of the parameters used to define repeating earthquakes in the Raukumara Peninsula study region. Based on this initial clustering, we extracted earthquakes within the region between −37.2° and −39.2° latitude and 177.2° and 179.7° longitude for further analysis. This region contained 133 possible repeating earthquake families. For each of these 133 possible families, we conducted manual phase picking of P- and S-arrivals for the youngest event in the family, hereafter referred to as the *core* event, to ensure consistent phase pick quality for the later analysis.

2.2. Repeating Earthquake Detection

The basis of our detection criterion is a threshold based on the cross-correlation of different events recorded at different stations. We assessed the sensitivity of the repeating earthquake catalog to variations in the length of the cross-correlation window, waveform filtering parameters, and the specific correlation threshold employed. We also compared our cross-correlation-derived catalog with one constructed using coherence as a measure of similarity (as used by some studies, e.g., Materna et al., 2018, see Figure S1 for comparison of methods). We chose not to use coherence as our detection metric because it introduced additional parameters, namely the frequency band over which coherence was assessed, without significantly changing our results.

We correlated waveforms for all stations that we were able to make manual P-phase picks on within the regional set of stations shown in Figure 2. A cross-correlation window length of 40 s, encompassing both P- and S-arrivals, has commonly been used in studies elsewhere to detect repeating earthquakes (Uchida, Hasegawa, et al., 2004; Uchida, Matsuzawa, Hasegawa, et al., 2003; Yamashita et al., 2012). However, because the event-to-station path-length in our study area varies between <10 and ∼180 km, S–P times and

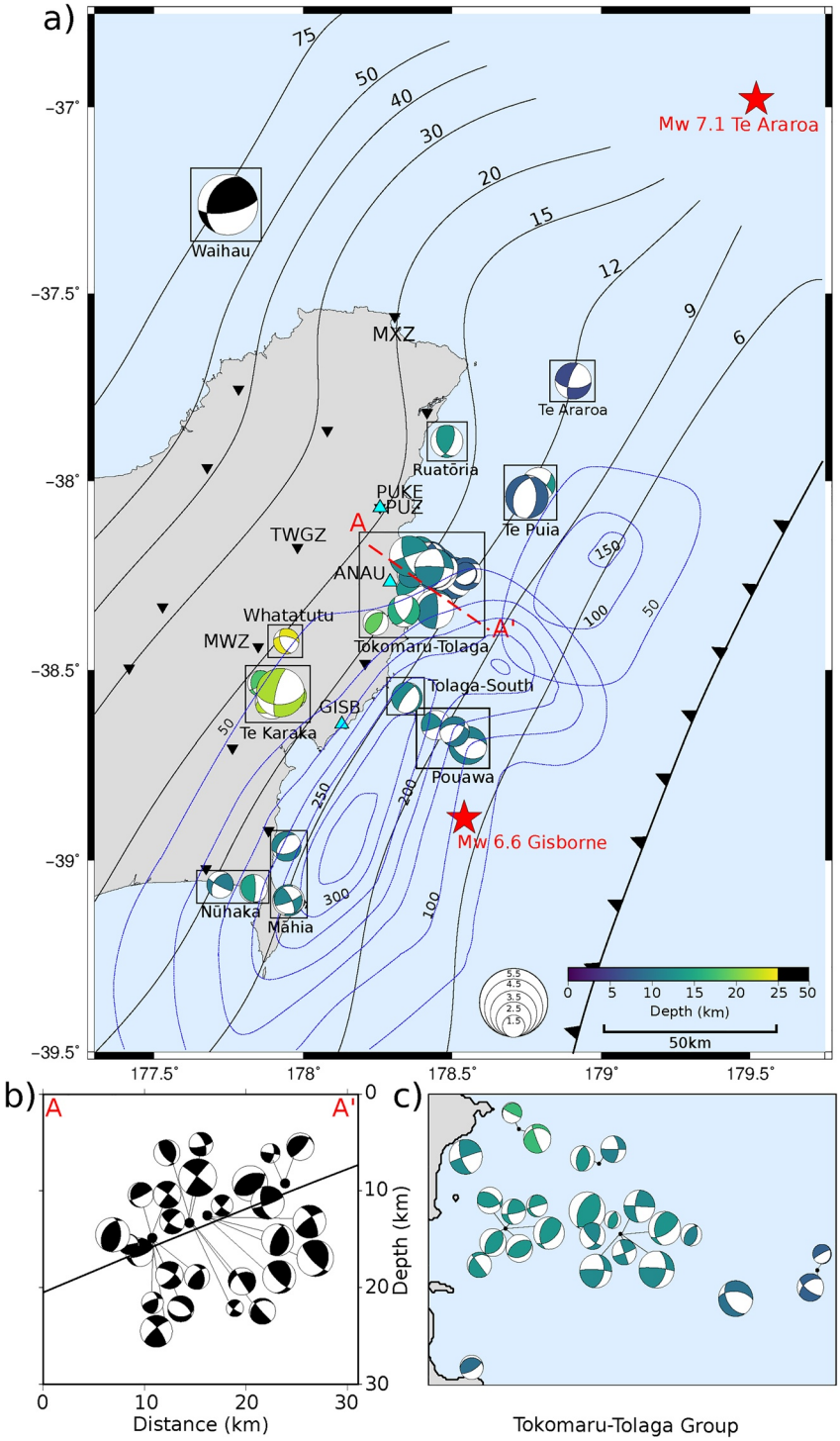

Figure 2. Maps (a, c) and cross-section (b) of repeating earthquake families focal mechanisms. (a) The repeating earthquakes are colored by depth and scaled by the calculated magnitudes. The red dashed line labeled A–A′ represents the location of the cross-section in (b). Contours mark the depth to the subduction interface modeled by C. A. Williams et al. (2013). Black inverted triangles mark the GeoNet seismic stations used to calculate the hypocenter locations. Data from the labeled stations are plotted in Figure 3. Blue contours demarcate slow-slip patches identified by Wallace and Beavan (2010) and Koulali et al. (2017) and are labeled in mm. Red stars mark the locations of the Gisborne M_W 6.6 earthquake and the Te Araroa M_W 7.1 earthquake. (b) Cross-section of the line A–A′, displaying seismicity with a ±10 km swath. (c) Expanded view of the Tokomaru–Tolaga group families' focal mechanism locations. *Note.* The maps in (a) and (c) show lower hemisphere projections and the cross-section in (b) shows back hemisphere projections.

coda durations also varied strongly between different events and different stations. We therefore chose to use a waveform length dependent on coda duration to compute robust cross-correlations that captured similar amounts of signal for different event-station paths. We found that using 75% of the coda duration (defined herein as when the signal-to-noise ratio first dropped below 1.5 and remained below this level for at least 0.5 s) was appropriate for calculating the normalized cross-correlation, as it includes both P- and S-arrivals and most of the coda, and resulted in the maximum normalized cross-correlation for visibly similar events. When the cross-correlation window length was less than 50% or greater than 100% of the coda length, the resulting cross-correlation between earthquakes in the prospective families was found to be distinctly lower. If we could not identify the end of the coda, due to the level of noise in the waveform, a window length of 25 s was imposed. In all cases, our cross-correlation windows started 1 s before the identified P-arrival. Cross-correlations were computed after aligning the waveforms on the P-arrivals, with each waveform allowed to shift by as much as 1 s to achieve optimal alignment and thereby allow the maximum cross-correlation to be calculated. We computed final cross-correlations using the multi-segment cross-correlation method suggested by Gao and Kao (2020) using four segments. We found that this better distinguished between repeating and nearby earthquakes when high-amplitude phases were recorded.

Prior to computing cross-correlations, we detrended the data and applied a fourth-order bandpass filter between 1 and 20 Hz. The lowcut of this filter was chosen to remove low-frequency noise found to dominate the signal at some of the broadband stations. We tested the response of the calculated normalized cross-correlation to changes in the highcut parameter but observed no strong variations and opted for a 20-Hz highcut as this retains a wide range of frequencies while ameliorating high-frequency noise.

Finally, to test the sensitivity of our catalog to changes in cross-correlation threshold, we determined which earthquakes would be retained as the correlation threshold was increased from 0.90 to 0.99 at intervals of 0.01. We required this threshold to be exceeded on at least two stations. We found that the number of families that were rejected as repeating and the number of events in each family varied more when the threshold was set to less than 0.95, compared to when it was larger than 0.95. When the threshold was set to greater than 0.95, families were rejected due to small differences in the background noise of the waveform rather than significant differences in the signal. We therefore chose to use a threshold of 0.95, as used in multiple other repeating earthquake studies (e.g., Uchida & Bürgmann, 2019, and references therein). We were unable to require high cross-correlation on more than two stations due to station continuity: nearby stations generally provide the highest cross-correlation values due to higher signal-to-noise ratios, but prior to 2003 there were only two permanent broadband seismometers and seven permanent short-period seismometers within 120 km of the main clusters of repeating earthquakes. This station continuity limits our analysis to times after 2003.

2.3. Location Procedure

We undertook absolute location and relative relocation of all possible repeating earthquakes to verify that events identified with the correlation-based detection criterion are indeed closely spaced. The phase picks in the original GeoNet catalog vary in quality, having been made using both automatic and manual methods, so we conducted additional phase picking for all events in our repeating earthquake catalog to ensure consistency. We manually picked P- and S-wave first arrivals for the core event in each family, which is commonly the best-recorded event due to the general increase with time of the number of stations, and identified P-wave polarities for later focal mechanism analysis. This yielded a total of 1,159 P-picks and 939 S-picks for the 133 possible families, resulting in an average of 9 P-picks and 7 S-picks for each of the core events. Fewer S-picks than P-picks were made due to the P coda obscuring the S-arrival at short epicentral distances. Since all events in a particular family are, by definition, well-correlated we were able to compute accurate (sub-sample) relative pick times for all the other events using the EQcorrscan cross-correlation pick correction function *xcorr_pick_family* (Chamberlain et al., 2018). This function follows the approach of Deichmann and Garcia-Fernandez (1992) and computes a moving window cross-correlation that is represented at each epoch by a parabolic function fit to the five samples around the maximum correlation. The peak of this parabola is taken as the time-shift of the pick. This workflow not only provides accurate and consistent phase arrivals but also provides 572 additional phase picks compared to the GeoNet catalog from which we started.

All the core events in our catalog have hypocenters computed by GeoNet but the location algorithms and velocity models with which they have been determined have changed throughout the catalog period. To generate consistent locations, and to take advantage of our additional phase picks, we computed absolute locations for all events using the NonLinLoc location software (Lomax et al., 2000) and the New Zealand-wide 3D velocity model (version 2.1) (Eberhart-Phillips & Bannister, 2015; Eberhart-Phillips, Bannister, et al., 2017). We also computed absolute locations using the SIMUL2014 software (Eberhart-Phillips, Reyners, et al., 2015) but found that this gave poorer fits to our picks compared to the NonLinLoc locations.

To test whether the earthquakes we identified as repeating based on correlation criteria truly overlap in source area, we also undertook relative relocation of all events. Due to the number and positions of seismometers in the network changing and generally improving with time, the absolute locations of older earthquakes are generally of poorer quality than the more recent earthquakes. To cope with this variable quality, and to test whether earthquakes within each family overlap, we used the absolute location of the core event in each family as the starting location for the relocation of all other events within the family. Using this starting location allows us to test whether the earthquakes within a family can be well-fit by overlapping locations, rather than necessarily providing highly accurate relative locations between families. For this relocation we used the GrowClust software of Trugman and Shearer (2017) with the onshore 1D velocity model from Yarce et al. (2019). Due to uncertainties in the relative relocations arising from variable station availability, our final composite criterion does not contain a condition requiring events in each family to have overlapping source areas to be identified as repeating earthquakes.

2.4. Focal Mechanisms

We constructed focal mechanisms for the core event in each family, using the manually picked P-wave first-motion polarities in the FPFIT (Reasenberg, 1985) routine implemented in SEISAN (Havskov & Ottemoller, 1999). P-wave first-motion polarities were picked on unfiltered waveforms. The event locations were fixed to the locations obtained using GrowClust, no relative weightings were applied to the polarities and a 2° increment was used to search for the best fit solution.

2.5. Matched-Filter Catalog Extension

To ensure continuity of our catalog, and to extend it beyond 2019 when we originally started our analysis, we used the core event identified in each family as templates in a matched-filter search spanning January 2003–January 2021, using the EQcorrscan package (Chamberlain et al., 2018). We constructed templates from data filtered between 1 and 20 Hz and resampled to 50 Hz for more efficient correlation computation. We cut templates to 25-s length starting 0.5 s before the P-pick for all available channels for all stations picked. These templates were correlated with continuous data downloaded from GeoNet, and processed in the same way as the templates.

We made detections when the average normalized cross-correlation across the network of stations used exceeded 0.5. We set a low initial threshold to ameliorate the effects of variable data quality across the network. We then computed cross-correlation pick-corrections, as outlined above, with a pick threshold of 0.8 normalized cross-correlation. We then fed the resulting detections back into our workflow to determine which of these detections were truly repeats. This extended our catalog to 347 earthquakes from an original set of 160 and confirmed that the final catalog of repeating events within each family does not depend on the completeness of the GeoNet catalog.

2.6. Magnitudes

Alongside variations in location procedure throughout the cataloged period, the magnitude-calculation procedures used by GeoNet have also varied. To generate consistent magnitudes we recomputed the local magnitudes of the core event in each family, and computed relative magnitudes for all other events within a family. To compute the magnitudes of the core events in each family we first generated automatic amplitude picks for the horizontal components of each station picked. Automatic amplitude picks were made on data that were filtered between 1 and 20 Hz, then instrument corrected and convolved with the

Table 1
Summary of the Repeating Earthquake Families Identified in Each of the Geographic Regions.

Geographic area	Abbreviated name	Number of families	T_{min}	T_{max}	M_{min}	M_{max}
Waihau	WA	1	6.2	6.2	5.1	5.2
Te Araroa	TA	1	1.7	1.7	2.3	2.6
Ruatōria	RA	2	1.9	3.8	2.2	2.4
Te Puia	TP	4	0.0	2.5	2.0	3.5
Tokomaru–Tolaga	TT	33	0.0	6.0	1.7	3.9
Whatatutu	WH	1	4.3	4.3	1.8	2.2
Tolaga South	TS	1	1.3	1.3	2.1	2.3
Te Karaka	TK	7	2.1	8.0	2.0	4.0
Pouawa	PO	5	1.3	4.0	2.0	3.4
Māhia	MA	4	1.1	6.7	1.9	3.1
Nūhaka	NU	2	1.3	1.6	1.9	2.3

Note. Geographic areas are identified in Figure 2. T_{min} and T_{max} are the minimum and maximum recurrence intervals, respectively, for each of the regional groups. M_{min} and M_{max} are the minimum and maximum local magnitudes, respectively, for each of the regional groups.

response of a Wood Anderson seismometer. The response of the pre-filter was subsequently corrected for in the resulting amplitude picks. The resulting amplitude picks were used to compute a consistent set of station correction and attenuation terms based on the GeoNet-computed local magnitudes for these events. The magnitudes for all other events within families were computed using a correlation-weighted average of the relative amplitudes, following the method of Schaff and Richards (2014).

3. Results

We identified 61 repeating earthquake families active between 2003 and 2020, which collectively contained 347 individual earthquakes. The 61 families are clustered into more active regions around the Raukumara Peninsula (Figure 2). To facilitate further description, we assigned each family to one of 11 regional groups, which were named based on their proximity to local population centers (see Figure 2). Within each of the regional groups, families were assigned a two letter geographic code and a two-digit number, based on the relative order of the first recorded repeating event in the family. The number of families within each of the regional groups ranges from 1 to 33 (Figure 2 and Table 1).

The repeating earthquake families identified have a magnitude range of M_L 1.7–5.2, and the recurrence intervals range between <1 and ∼7 yr (Table 1). The number of repeating events in each of the families ranges from 2 to 15. In Figure 3, the waveforms of the repeating events in four regional groups are depicted, highlighting the visual similarities between the events in each of the families. In Figure 3, WA01 is the largest magnitude family in the catalog and is the only family located to the northwest of the Raukumara Peninsula, TA01 is the furthest offshore family (∼30 km), TS01 locates ∼10 km offshore just south of Tolaga Bay and NU02 locates onshore to the west of the Māhia Peninsula.

Focal mechanism for 55 of the 61 families were constructed, with the remaining six families not having focal mechanism created due to a lack to first arrival polarities being identified during manual picking. The focal mechanisms of the repeating earthquake families are consistent with both upper and lower intra-plate faulting, as well as faulting along the subduction interface. Due to the location of the families with respect to the GeoNet seismic network (see Figure S2), many of the focal mechanisms are poorly constrained, with maximum one sigma errors for the strike, dip, and rake being 34.0°, 30.0°, and 54.0°, respectively. The average one sigma error in the strike, dip, and rake of the focal mechanisms are 7.06°, 8.67°, and 14.53°, respectively.

The magnitude of completeness of the GeoNet catalog around the Raukumara region varied from ∼M 3 in 2003 to ∼M 2 in 2019 (Figure 4a). In the Raukumara repeating earthquake catalog, only 17 of the 347 identified repeating earthquakes have calculated local magnitudes which are less than M_L 2 (Figure 4b). While the matched-filter results have ensured that the families presented here are complete over the 17-yr study, our set of families is intrinsically linked to the GeoNet catalog and may be missing smaller magnitude families that were not included in the GeoNet catalog.

4. Discussion

4.1. Spatial and Temporal Relationships to Other Subduction Phenomena

Based on the location of the core event and focal mechanism of each family, we categorized the repeating earthquakes as occurring on the subduction interface, within the Australian plate, or within the Pacific plate. Families which had a low-angle reverse focal mechanism and were within ∼5 km of the C. A. Williams et al. (2013) interface model were assumed to be occurring on the interface, or associated faults, and the remaining families were assigned to the over-riding or down-going plate based on their location relative

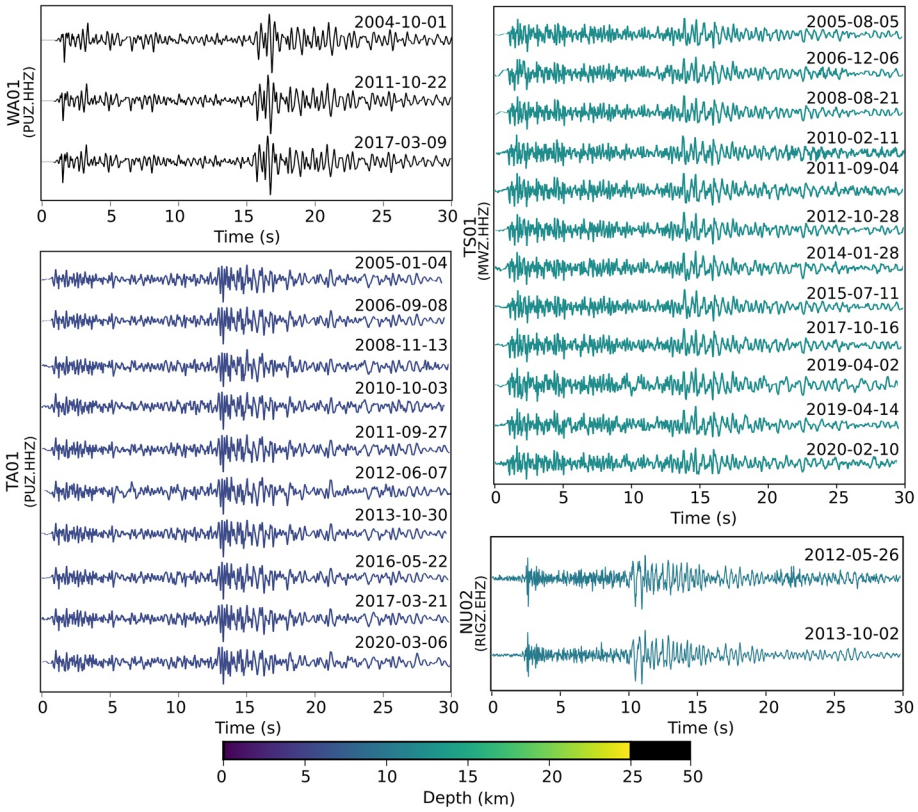

Figure 3. Representative repeating earthquake waveforms from four regional groups. All waveforms have had a fourth-order bandpass filter between 1 and 20 Hz applied. The GeoNet stations and channels that the waveforms were recorded on are included in the brackets under the family names. Waveforms are colored by earthquake depth. Top left: Waihau (WA) group family. Top right: Tolaga-South (TS) group family. Bottom left: Te Araroa (TA) group family. Bottom right: Nūhaka (NU) group family.

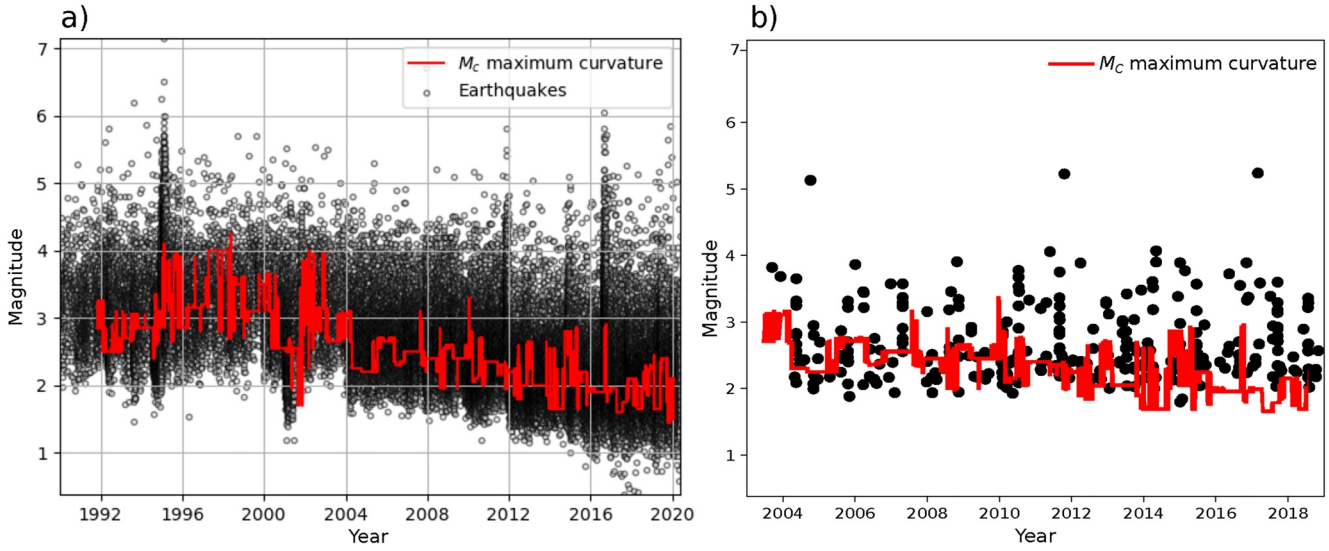

Figure 4. Magnitude of completeness for the repeating earthquake catalog. (a) Calculated magnitude of completeness of the GeoNet catalog around the Raukumara region, from 1992 to 2019. We calculated completeness using the maximum curvature method (Wiemer & Wyss, 2000) for groups of 2,000 events. (b) Calculated local magnitude of the repeating earthquakes identified in this catalog through time. Note the shortened time scale in (b).

to those events. As a result, 39 families are concluded to occur within the over-riding Australian Plate, exhibiting a range of faulting types, 15 occur along the subduction interface, and 7 are in the down-going Pacific Plate and exhibit predominantly strike-slip and normal faulting focal mechanisms. However, 35 of the families not concluded to occur on the plate interface, due to the type of faulting are located within ±5 km of the interface (Figure 5). While the focal mechanism of WA01 is consistent with interface faulting, the mean depth (58 km) of the family is slightly shallower than the interface model (c. 70 km), so is not considered consistent with being on the interface.

All of the repeating earthquake families inferred, on the basis of their hypocenters and focal mechanisms, to occur on the subduction interface lie within regions identified by Wallace, Beavan, Bannister, et al. (2012) to have low coupling (Figure 5). The spatial relationship of the intra-plate families to interface locking is less clear, with only the Pouawa and Tolaga-South families located above, and below, the locked–sliding transition.

Heise et al. (2017) recently investigated the relationship between geodetically observed locking of the subduction interface (Dimitrova et al., 2016; Wallace, Beavan, Bannister, et al., 2012) and the physical properties of the interface inferred from electrical resistivity observations. They argued that areas in which the interface is locked and the upper plate is undergoing areal contraction are electrically resistive, notably between the Māhia Peninsula and Tolaga Bay, and concluded that the frictional coupling of the interface is governed by low fluid or sediment volumes.

We observe that repeating earthquake families occurring on the subduction interface and in the over-riding plate in the Te Karaka group coincide with an area of distinctively high resistivity on and above the interface (200–600 Ωm) identified by Heise et al. (2017); the single family in Whatatutu group, which occurs in the Pacific plate, lies beneath this zone of high resistivity. However, repeating earthquakes occurring on the interface or in the upper plate in the Māhia and Nūhaka groups in the south of the Peninsula and the Tolaga Bay and Tokomaru Bay groups further north occur within zones of relatively low interface resistivity (≤20 Ωm; cf. Figure 2 of Heise et al., 2017). Moreover, no clear spatial relationship is evident between the epicenters of repeating earthquakes and areal strain rates (Figure 4 of Dimitrova et al., 2016).

Active-source seismic imaging has revealed two seamounts subducting offshore between the Māhia Peninsula and Tokomaru Bay (Figure 5, after Bell, Sutherland, et al., 2010). In addition, high-amplitude reflections have been observed adjacent to the plate interface, down-dip of the subducting seamounts (Bell, Sutherland, et al., 2010). Bell, Sutherland, et al. (2010) interpreted these high-amplitude reflections as fluid-rich sediments, entrained by the subducting seamount. The Pouawa group families (offshore to the southeast of Tolaga Bay) are located down-dip of the southern seamount, coincident with the high-amplitude reflectors mapped by Bell, Sutherland, et al. (2010) and down-dip of the "burst–type" repeating earthquakes identified by Shaddox and Schwartz (2019), but no repeating earthquakes have been detected in the vicinity of the northern seamount.

When the location of the repeating earthquakes are compared to the location of previously identified slow slip, the Te Karaka, Whatatutu, Tokomaru–Tolaga, and Te Puia (TP) groups locate along the down-dip periphery of the identified cumulative slow-slip patch (Figure 2; Koulali et al., 2017; Wallace & Beavan, 2010; Wallace, Webb, et al., 2016). In comparison, the Nūhaka and Māhia repeating earthquakes transect the southern extent of the modeled slow-slip patch (Wallace & Beavan, 2010; Wallace, Webb, et al., 2016). Furthermore, the Pouawa and Tolaga-South group families lie along the boundary between two persistent patches of slow-slip, which occur to the northeast and southwest of the families locations (Wallace & Beavan, 2010; Wallace, Webb, et al., 2016).

We next consider the temporal relationships between the repeating earthquakes and previously described slow-slip. Such relationships have been extensively documented throughout the Japan subduction zone (Gardonio et al., 2018; Igarashi et al., 2003; Kato et al., 2012; Uchida, Hasegawa, et al., 2004; Uchida, Iinuma, et al., 2016; Uchida & Matsuzawa, 2013; Uchida, Matsuzawa, Hirahara, et al., 2006) and we similarly compare the timing of individual repeating earthquakes and their cumulative moment release to time-series of geodetically measured displacement and recognized episodes of slow-slip (Figure 6). For the purposes of comparison with measured deformation, we focus on the displacement time-series from GeoNet's global navigation satellite system station near Gisborne ("GISB") as it provides a general reference for motion in

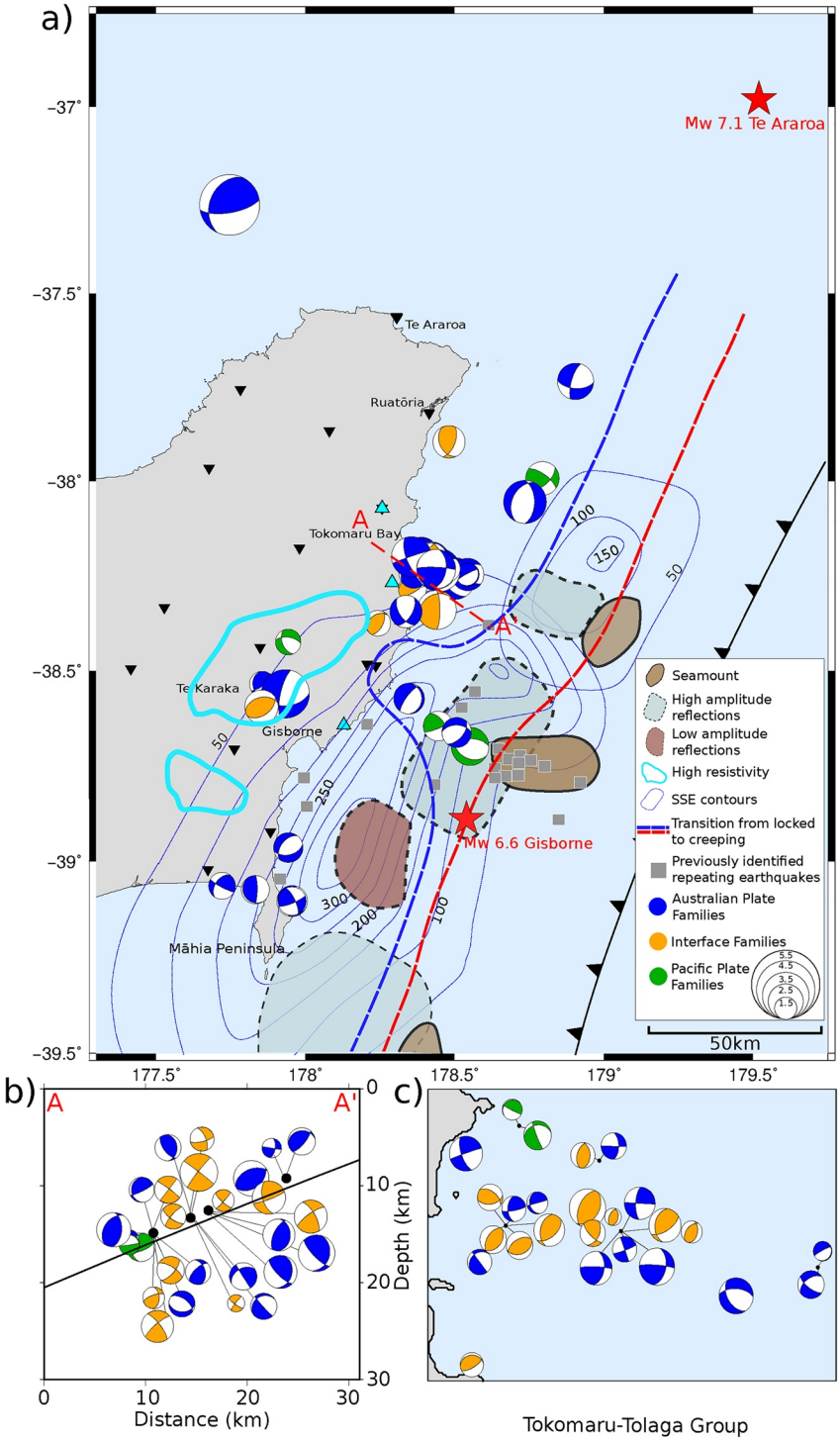
a)
Mw 7.1 Te Araroa
Te Araroa
Ruatōria
Tokomaru Bay
A
A'
Te Karaka
Gisborne
Mw 6.6 Gisborne
Māhia Peninsula
100
150
50
250
300
200
Seamount
High amplitude reflections
Low amplitude reflections
High resistivity
SSE contours
Transition from locked to creeping
Previously identified repeating earthquakes
Australian Plate Families
Interface Families
Pacific Plate Families
50km
-37°
-37.5°
-38°
-38.5°
-39°
-39.5°
177.5°
178°
178.5°
179°
179.5°
b)
Distance (km)
Depth (km)
c)
Tokomaru-Tolaga Group

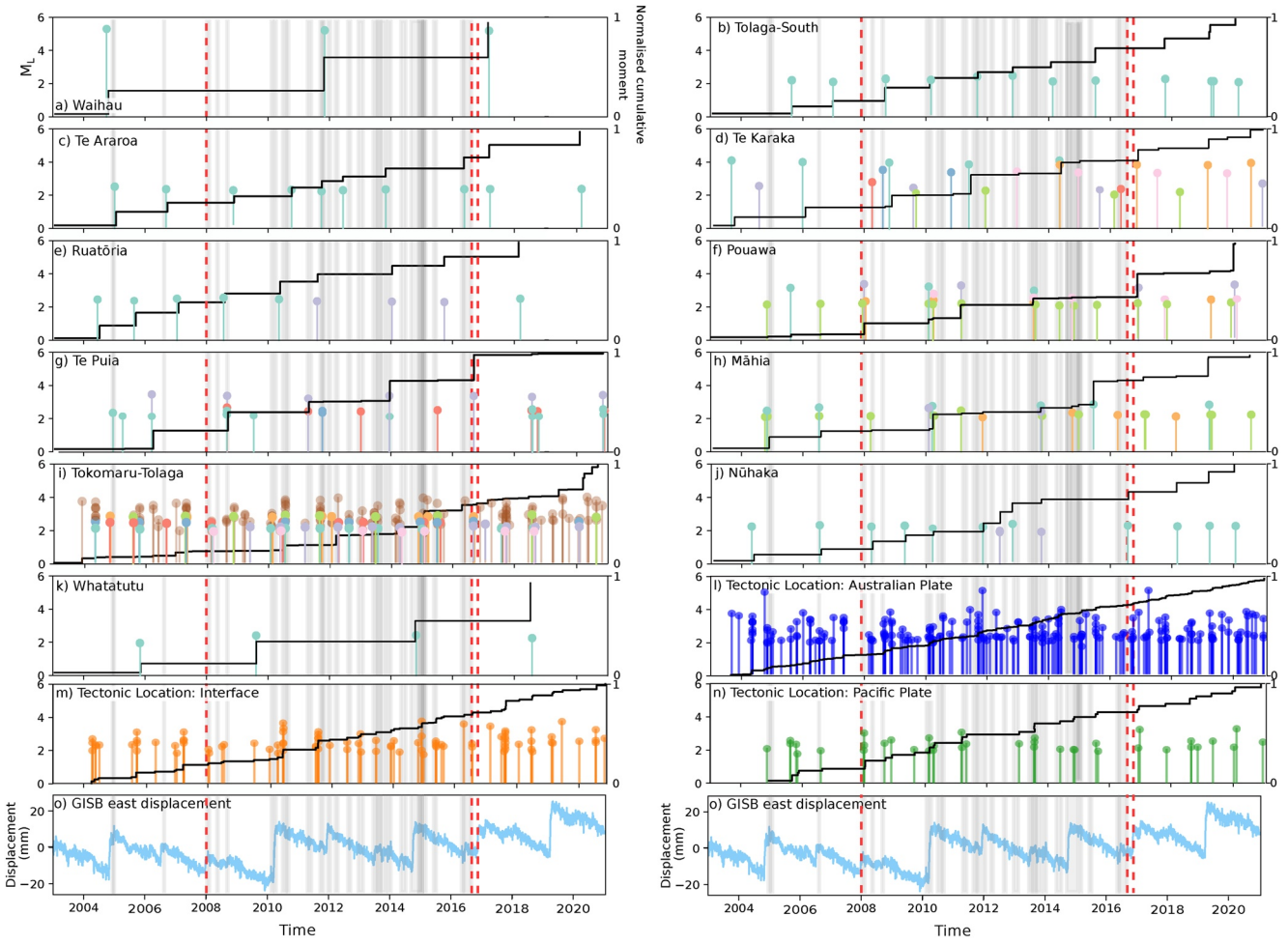

Figure 6. Chronology of repeating earthquakes and cumulative moment release within each geographic area. The lollipop symbols indicate the timing and magnitude of each repeating earthquake and are colored by family. For geographic areas containing more the seven families, the largest seven families are distinguished by different colors and the remaining events are colored brown to show their occurrence. Panels l), m) and n) depict the timing of the repeating earthquakes colored by their tectonic location. Episodes of slow slip periods (Koulali et al., 2017; Todd & Schwartz, 2016; Wallace & Beavan, 2010; Wallace, Beavan, Bannister, et al., 2012; Wallace & Eberhart-Phillips, 2013; Wallace, Webb, et al., 2016) are shown in gray and large earthquakes are marked in red. Note that the slow-slip catalog completeness is not consistent in time. The panels (o) and (p) show the east-component from the GISB (Gisborne) GNSS site operated by GeoNet and are repeated to aid visual comparisons. The cumulative moment curves are normalized to unity for comparison between different regional groups.

the region of interest and has been operating continuously since 2002. We compute the moment of each repeating earthquake by converting the calculated local magnitudes using the following scaling relationship in Aki (1972).

$$\log(M_0) = 1.4\log(M_L) + 17.0 \quad (1)$$

Figure 5. Maps (a, c) and cross-section (b) of repeating earthquake families tectonic locations. (a) Locations of the Raukumara Peninsula repeating earthquake families colored according to whether an event is occurring in the Australian Plate, along the interface or within the Pacific Plate, and scaled by calculated magnitude. The red dashed line labeled A–A′ represents the location of the cross-section in (b). Blue contours demarcate slow-slip patches identified by Wallace and Beavan (2010) and Koulali et al. (2017) and are labeled in mm. Blue and red dashed lines identify the transition from locked to creeping regions of the geodetic locking model of Wallace, Beavan, Bannister, et al. (2012). The interface is locked to the right of the red line and creeping to the left of the blue line. Seamount locations and high- and low-amplitude reflections are adapted from Bell, Sutherland, et al. (2010), and the regions of the interface which have a high resistivity (200–600 Ωm) are illustrated after Heise et al. (2017). "Burst-type" repeating earthquakes identified by Shaddox and Schwartz (2019) are shown in gray squares. Red stars mark the locations of the Gisborne M_W 6.6 earthquake and the Te Araroa M_W 7.1 earthquake. (b) Cross-section of the line A–A′, displaying seismicity with a ±10 km swath. (c) Expanded view of the Tokomaru–Tolaga group families' focal mechanism locations. *Note*. The maps in (a) and (c) show lower hemisphere projections and the cross-section in (b) shows back hemisphere projections.

We observe some episodes of slow-slip to be accompanied by repeating earthquake activity in some families, such as in 2004 (TA and TP groups) and in 2011 (TA and TP groups again) (Figure 6). However, this is not consistent for all SSEs or regional repeating earthquake groups. Of the 31 SSEs previously identified to the north of Māhia Peninsula, all coincide with the occurrence of repeating earthquakes. The Ruatōria and Pouawa groups show the clearest correlation between the occurrence of the repeating earthquakes and the occurrence of an SSE (Figures 6e and 6f, respectively). For the Ruatōria group, four of the nine repeating earthquakes occur during the approximate timing of the SSEs that occurred after 2004, with the SSEs occurring from the Māhia Peninsula to Puketiti (Figure 6e). Moreover, 18 events in the Pouawa group correspond to the occurrence of SSEs, with four of these SSEs occurring around Gisborne. In general, we note the apparent clustering of our repeating earthquakes, which may be indicative of a shared underlying driving stress, or/and interaction between families.

Distinguishing the repeating earthquakes on the basis of tectonic position (Figure 6m) reveals marked steps in the cumulative moment release of earthquakes occurring on the subduction interface at the time of slow slip in early 2010. The early 2010 episode of slow slip occurred between Tolaga Bay and Māhia (Wallace & Beavan, 2010). The two largest increments of moment release associated with Pacific Plate repeating earthquakes occurred in late 2005 and early 2011 and neither is associated with recognized slow slip. Australian Plate repeating earthquakes exhibit a generally constant rate of moment release with the largest increments showing no clear relationship to episodes of slow slip.

Jacobs et al. (2016) analyzed seismicity associated with SSEs along the length of the Hikurangi subduction margin and found that three of the largest sequences occurred in 2007, 2009, and 2010 approximately 20 km to the east of the Raukumara Peninsula. We observe increases in the number of repeating earthquakes occurring in the Australian Plate at the times of both the 2009 and 2010 sequences but not the 2007 sequence. Similar patterns are observed with the Pacific Plate and interface families, with the rate of repeating earthquakes increasing in response to the 2010 sequence but not the 2007 or 2009 sequences. The patterns we have observed are consistent with the findings of Delahaye et al. (2009), who identified microearthquakes occurring either on the subduction interface or just below that were triggered down-dip of an SSE in October–November 2004. The repeating earthquakes families also occur in similar locations to the microseismicity identified by Yarce et al. (2019), with only one repeating earthquake family (TS01) occurring in a seismicity gap identified in that study. Moreover, work done by Bassett et al. (2014), to try and explain the occurrence of slow-slip in the region, identified slower wavespeeds and the possibility of near-lithostatic fluid pressures on the interface, which may also have an effect on the repeating earthquakes, alongside inferred fluid-pressure cycling related to SSE occurrence (Warren-Smith, Fry, Wallace, et al., 2019).

We also compared the timing of three large regional earthquakes to the occurrence of repeating earthquakes. Two of these earthquakes occurred within the area of interest around the Raukumara Peninsula. The first was the M_W 6.6 Gisborne earthquake, which occurred on December 20, 2007, UTC, 64 km from Gisborne at a depth of 40 km, in the subducting Pacific Plate (Francois-Holden et al., 2008). The second was the M_W7.1 TA earthquake, which occurred on September 1, 2016, UTC, at a depth of 19 km, also in the subducting Pacific Plate (Warren-Smith, Fry, Kaneko, et al., 2018). The timing of the 2016 M_W 7.8 Kaikōura earthquake was also compared to the timing of repeating earthquakes despite not occurring within the study area, as it is known to have triggered slow-slip in the study region (Wallace, Hreinsdóttir, et al., 2018). We observe a step in cumulative moment in three of the regional groups following these three large earthquakes. The Pouawa group is the only regional group for which steps in the cumulative moment are observed following to the Gisborne M_W 6.6 earthquake, occurring 5 months following the event, as well as a step 19 days after the Kaikōura earthquake (Figure 6f). Three days following Kaikōura earthquake, a step in the Tokomaru–Tolaga group is also observed (Figure 6i). Moreover, the TP group is the only regional group which showed a step in the cumulative moment following the TA earthquake (Figure 6f). We see no evidence for direct triggering of repeating earthquakes following these large earthquakes.

In summary, 39 families are concluded to occur within the over-riding Australian Plate, 15 occur along the subduction interface and 7 are in the down-going Pacific Plate. All of the repeating earthquake families inferred to occur on the subduction interface lie within regions identified by Wallace, Beavan, Bannister, et al. (2012) to have low coupling. We observe that families in the Te Karaka and Whatatutu groups coincide with an area of distinctively high resistivity (200–600 Ωm; Heise et al., 2017), and the Pouawa group families

are located down-dip of a subducting seamount, coincident with high-amplitude reflectors mapped by Bell, Sutherland, et al. (2010). The repeating earthquakes show little consistent response to any of the SSEs previously identified or the three large earthquakes that have occurred in the time spanned by this study. However, for nine of the 11 regional groups we observe repeating earthquakes occurring during periods of slow-slip and following large regional earthquakes (Koulali et al., 2017; Todd & Schwartz, 2016; Wallace & Beavan, 2010; Wallace, Beavan, Bannister, et al., 2012; Wallace & Eberhart-Phillips, 2013; Wallace, Webb, et al., 2016). Finally, the patterns we have observed in repeating earthquakes are similar to those of seismicity sequences observed by Jacobs et al. (2016) associated with SSEs and microseismicity observed by Delahaye et al. (2009) and Yarce et al. (2019).

4.2. Scaling Relationships for Raukumara Peninsula Repeating Earthquakes

Nadeau and Johnson (1998) proposed that the magnitudes of repeating earthquakes should scale as a function of recurrence interval, based on the cyclic loading and stress release model. They demonstrated this to be the case near Parkfield, California, obtaining the relationship:

$$\log(T) = 4.85 + 0.17\log(M_O) \tag{2}$$

where T is the recurrence interval in seconds and M_O is the seismic moment in dyne-cm. This scaling of moment with recurrence interval has since been examined and verified in other many other locations (Chen & Lapusta, 2009; Chen et al., 2007; Dominguez et al., 2016; Johnson, 2010; Lengliné & Marsan, 2009; Marone et al., 1995; Mavrommatis et al., 2015; Mesimeri & Karakostas, 2018; Nadeau & Johnson, 1998; Peng et al., 2005; Schaff & Richards, 2011; Uchida, 2019; Yu, 2013). Slight variations in the relationship have been observed between different regions, as have changes in scaling before and after nearby large earthquakes (Chaves et al., 2020; Schaff & Richards, 2011; Yu, 2013).

To investigate this relationship in the New Zealand context, we used the average recurrence interval for each of the repeating earthquake families and the moment of the core event in the family (Figure 7). The magnitude of the core event was taken to represent each family as a whole, rather than averaging the values of all the events in a family, for two reasons: first, the magnitudes of each of the families were extremely similar; and second, it was assumed that the core event in each family had the best-constrained magnitude and lowest associated error due to overall improvements in network coverage and geometry.

In Figure 7, families with durations shorter than 6 months ($n = 2$) were removed before the relationships were calculated, as the relationship identified by Nadeau and Johnson (1998) was for long duration repeating earthquake families, and we wanted to compare similar families. Furthermore, these short duration families masked any identifiable relationship between recurrence interval and seismic moment. As can be seen in Figure 7, the relationship between seismic moment and recurrence interval for the Raukumara Peninsula repeating earthquake families is weaker than the relationship identified by Nadeau and Johnson (1998). However, the 95% confidence intervals for both the gradient and the intercept include the values for the Parkfield repeating earthquakes. Due to the scatter in the data for all the plate locations, the confidence intervals are extremely wide, and prevent us from determining a reliable relationship. Overall, while we found that the Raukumara Peninsula repeating earthquake families' relationship between recurrence interval and seismic moment followed a weakly positive trend, consistent with the findings of repeating earthquake studies elsewhere, the uncertainty associated with these trends is very large. This places uncertainty on applying other relationships established by Nadeau and Johnson (1998) to the Raukumara Peninsula repeating earthquakes. We speculate that the scatter we observe may be due to the influence of variable slip-rates associated with nearby slow-slip episodes.

4.2.1. Calculating the Slip-Rate of the Repeating Earthquake Families

Using 53 repeating earthquake families, from the Parkfield segment of the San Andreas fault, and 8 repeating earthquake families from the Stone Canyon section, Nadeau and Johnson (1998) derived a formula which relates the average seismic moment to the average amount of slip of a repeating earthquake family (Equation 3). The Parkfield segment families had a magnitude range of M_W −0.7 to 1.4, while the Stone Canyon families were added to the analysis to extend the magnitude range to M_W 3.7–6.0. Nadeau and Johnson (1998) derived the relationship:

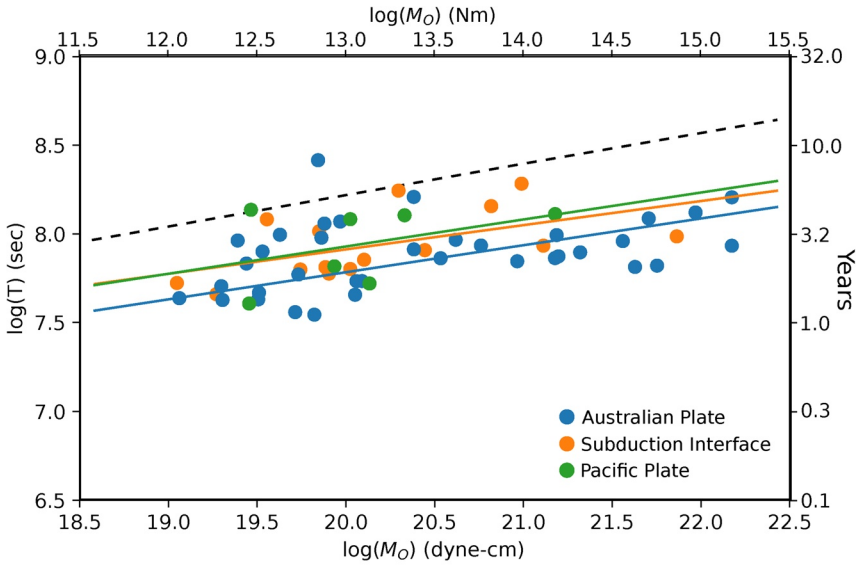

Location	Intercept	Gradient
Australian Plate	4.94 (0.31 - 7.51)	0.14 (0.01 - 0.37)
Interface	5.16 (2.47 - 10.47)	0.14 (-0.13 - 0.27)
Pacific Plate	4.86 (-0.89 - 7.11)	0.15 (0.03 - 0.47)
Parkfield (Nadeau and Johnson, 1998)	4.85 ± 0.16	0.17± 0.009

Figure 7. Repeating earthquake recurrence interval–seismic moment relationship. Top: Raukumara Peninsula repeating earthquake families' average recurrence interval plotted against seismic moment and colored according to occurrence in the overlying Australian Plate, on the subduction interface or in the subducting Pacific Plate. Shown in the black dashed line is the relationship obtained for repeating earthquakes near Parkfield, California, by Nadeau and Johnson (1998). Linear relationships of the logarithms of each of the variables were fitted by minimizing the L2 norm, after families with durations shorter than 6 months had been removed. Bottom: intercept and gradient values, including the 95% confidence intervals for the recurrence interval seismic moment relationships plotted above. The relationship identified by Nadeau and Johnson (1998) has been included for comparison.

$$\log(d) = -2.36 + 0.17\log(M_O) \tag{3}$$

where d is the average amount of slip for a repeating earthquake family in cm, and M_O is the average seismic moment of the repeating earthquake family, in dyne-cm. This relationship has also been applied to other tectonic setting and studies, including Japan, to determine the slip of identified repeating earthquake families (Uchida, Matsuzawa, Hasegawa, et al., 2003). Based on the magnitude range the relationship was derived over, and that it has been universally applied to different settings, we applied the relationship to the Raukumara Peninsula repeating earthquake families, to calculate the slip-rate.

Preliminary slip-rates calculated for the Raukumara Peninsula repeating earthquake families range from <10 up to ~60 mm/yr, when the families with extremely short family durations (less than 1 yr) are excluded. Generally, the shorter the family duration the faster the slip-rate will be. This trend follows previously established relationships for Parkfield and Japan, with short duration families having slip-rates which are significantly higher than the tectonic loading rate, compared to long-duration families. However, due to the differences observed in the seismic moment–recurrence interval relationship previously mentioned, applying the Parkfield repeating earthquake slip model to the Raukumara Peninsula families, may not be appropriate.

5. Conclusions

We have identified 61 repeating earthquake families containing a total of 347 earthquakes that occurred between 2003 and 2020 in the vicinity of the Raukumara Peninsula, on the northern Hikurangi subduction margin. These families represent a range of faulting types and occur along the subduction interface and in

the overlying and subducting plates. We observe steps in the cumulative moment of the repeating earthquakes coinciding with all of 31 previously identified SSEs. We also compared the Raukumara Peninsula families to families and repeating earthquake relationships previously identified around Parkfield, California. When comparing recurrence interval–seismic moment relationships, we identified a similar trend between the two locations, however when calculating the slip-rate of the families, no interface families were found to have an estimated slip-rate that matched the plate convergence rate.

Data Availability Statement

All waveform and input event data are available from the New Zealand GeoNet project, and can be accessed at https://www.geonet.org.nz/data/tools/FDSN (last accessed April 16 2021). Results from this paper are included in the supplementary material.

Acknowledgments
We gratefully acknowledge funding provided by the Marsden Fund of the Royal Society Te Apārangi (project 17-VUW-121) and the Earthquake Commission Program in Seismology and Tectonic Geodesy at Victoria University of Wellington–Te Herenga Waka. We also acknowledge the New Zealand GeoNet project and its sponsors EQC, GNS Science, and LINZ, for providing the data used in this study (which can be accessed at https://www.geonet.org.nz/data/tools/FDSN), last accessed July 26, 2019). The figures in this article were constructed using the Generic Mapping Tools (Wessel et al., 2019), matplotlib (Hunter, 2007), and ObsPy (Beyreuther et al., 2010). We acknowledge GNS Science for maintaining and providing access to the New Zealand Active Faults Database through the website data.gns.cri.nz/af/ (last accessed 3 December 2020). We are grateful for constructive reviews by two anonymous reviewers, and editor Maureen Long.

References

Abercrombie, R. E., Chen, X., & Zhang, J. (2020). Repeating earthquakes with remarkably repeatable ruptures on the San Andreas Fault at Parkfield. *Geophysical Research Letters*, *47*(23), e2020GL089820. https://doi.org/10.1029/2020GL089820

Aki, K. (1972). Scaling law of earthquake source time-function. *Geophysical Journal International*, *31*(1–3), 3–25. https://doi.org/10.1111/j.1365-246x.1972.tb02356.x

Barnes, P. M., Lamarche, G., Bialas, J., Henrys, S., Pecher, I., Netzeband, G. L., et al. (2010). Tectonic and geological framework for gas hydrates and cold seeps on the Hikurangi subduction margin, New Zealand. *Marine Geology*, *272*(1–4), 26–48. https://doi.org/10.1016/j.margeo.2009.03.012

Bassett, D., Sutherland, R., & Henrys, S. (2014). Slow wavespeeds and fluid overpressure in a region of shallow geodetic locking and slow slip, Hikurangi subduction margin, New Zealand. *Earth and Planetary Science Letters*, *389*, 1–13. https://doi.org/10.1016/j.epsl.2013.12.021

Beanland, S. (1995). *The North Island dextral fault belt, Hikurangi subduction margin*. (Doctoral dissertation, Victoria University of Wellington, New Zealand) [in Geology].

Bell, R., Holden, C., Power, W., Wang, X., & Downes, G. (2014). Hikurangi margin tsunami earthquake generated by slow seismic rupture over a subducted seamount. *Earth and Planetary Science Letters*, *397*, 1–9. https://doi.org/10.1016/j.epsl.2014.04.005

Bell, R., Sutherland, R., Barker, D. H. N., Henrys, S., Bannister, S., Wallace, L., & Beavan, J. (2010). Seismic reflection character of the Hikurangi subduction interface, New Zealand, in the region of repeated Gisborne slow slip events. *Geophysical Journal International*, *180*(1), 34–48. https://doi.org/10.1111/j.1365-246x.2009.04401.x

Beyreuther, M., Barsch, R., Krischer, L., Megies, T., Behr, Y., & Wassermann, J. (2010). ObsPy: A Python toolbox for seismology. *Seismological Research Letters*, *81*(3), 530–533. https://doi.org/10.1785/gssrl.81.3.530

Bohnhoff, M., Wollin, C., Domigall, D., Küperkoch, L., Martínez-Garzón, P., Kwiatek, G., et al. (2017). Repeating Marmara Sea earthquakes: indication for fault creep. *Geophysical Journal International*, *210*(1), 332–339. https://doi.org/10.1093/gji/ggx169

Chamberlain, C. J., Hopp, C. J., Boese, C. M., Warren-Smith, E., Chambers, D., Chu, S. X., et al. (2018). EQcorrscan: Repeating and near-repeating earthquake detection and analysis in Python. *Seismological Research Letters*, *89*(1), 173–181. https://doi.org/10.1785/0220170151

Chaves, E. J., Schwartz, S. Y., & Abercrombie, R. E. (2020). Repeating earthquakes record fault weakening and healing in areas of megathrust postseismic slip. *Science Advances*, *6*(32), eaaz9317. https://doi.org/10.1126/sciadv.aaz9317

Chen, K. H., Bürgmann, R., & Nadeau, R. M. (2013). Do earthquakes talk to each other? Triggering and interaction of repeating sequences at Parkfield. *Journal of Geophysical Research: Solid Earth*, *118*(1), 165–182. https://doi.org/10.1029/2012jb009486

Chen, K. H., Bürgmann, R., Nadeau, R. M., Chen, T., & Lapusta, N. (2010). Postseismic variations in seismic moment and recurrence interval of repeating earthquakes. *Earth and Planetary Science Letters*, *299*(1–2), 118–125. https://doi.org/10.1016/j.epsl.2010.08.027

Chen, K. H., Nadeau, R. M., & Rau, R. (2007). Toward a universal rule on the recurrence interval scaling of repeating earthquakes? *Geophysical Research Letters*, *34*(16), 1–5. https://doi.org/10.1029/2007gl030554

Chen, K. H., Nadeau, R. M., & Rau, R.-J. (2008). Characteristic repeating earthquakes in an arc-continent collision boundary zone: The Chihshang fault of eastern Taiwan. *Earth and Planetary Science Letters*, *276*(3–4), 262–272. https://doi.org/10.1016/j.epsl.2008.09.021

Chen, T., & Lapusta, N. (2009). Scaling of small repeating earthquakes explained by interaction of seismic and aseismic slip in a rate and state fault model. *Journal of Geophysical Research: Solid Earth*, *114*(B1), 1–12. https://doi.org/10.1029/2008jb005749

Clark, K., Howarth, J., Litchfield, N., Cochran, U., Turnbull, J., Dowling, L., et al. (2019). Geological evidence for past large earthquakes and tsunamis along the Hikurangi subduction margin, New Zealand. *Marine Geology*, *412*, 139–172. https://doi.org/10.1016/j.margeo.2019.03.004

Deichmann, N., & Garcia-Fernandez, M. (1992). Rupture geometry from high-precision relative hypocentre locations of microearthquake clusters. *Geophysical Journal International*, *110*(3), 501–517. https://doi.org/10.1111/j.1365-246x.1992.tb02088.x

Delahaye, E. J., Townend, J., Reyners, M. E., & Rogers, G. (2009). Microseismicity but no tremor accompanying slow slip in the Hikurangi subduction zone, New Zealand. *Earth and Planetary Science Letters*, *277*(1–2), 21–28. https://doi.org/10.1016/j.epsl.2008.09.038

Dimitrova, L., Wallace, L., Haines, A., & Williams, C. (2016). High-resolution view of active tectonic deformation along the Hikurangi subduction margin and the Taupo Volcanic Zone, New Zealand. *New Zealand Journal of Geology and Geophysics*, *59*(1), 43–57. https://doi.org/10.1080/00288306.2015.1127823

Dominguez, L. A., Taira, T. a., & Santoyo, M. A. (2016). Spatiotemporal variations of characteristic repeating earthquake sequences along the Middle America Trench in Mexico. *Journal of Geophysical Research: Solid Earth*, *121*(12), 8855–8870. https://doi.org/10.1002/2016jb013242

Doser, D. I., & Webb, T. H. (2003). Source parameters of large historical (1917–1961) earthquakes, North Island, New Zealand. *Geophysical Journal International*, *152*(3), 795–832. https://doi.org/10.1046/j.1365-246x.2003.01895.x

Douglas, A., Beavan, J., Wallace, L., & Townend, J. (2005). Slow slip on the northern Hikurangi subduction interface, New Zealand. *Geophysical Research Letters*, *32*(16), 1–4. https://doi.org/10.1029/2005gl023607

Eberhart-Phillips, D., & Bannister, S. (2015). 3-D imaging of the northern Hikurangi subduction zone, New Zealand: Variations in subducted sediment, slab fluids and slow slip. *Geophysical Journal International*, *201*(2), 838–855. https://doi.org/10.1093/gji/ggv057

Eberhart-Phillips, D., Bannister, S., & Reyners, M. (2017). New Zealand Wide model 2.1 seismic velocity model for New Zealand. *Zenodo*. https://doi.org/10.5281/zenodo.1043558

Eberhart-Phillips, D., Reyners, M., & Bannister, S. (2015). A 3DQPAttenuation model for all of New Zealand. *Seismological Research Letters*, *86*(6), 1655–1663. https://doi.org/10.1785/0220150124

François-Holden, C., Bannister, S., Beavan, J., Cousins, J., Field, B., McCaffrey, R., et al. (2008). The Mw 6.6 Gisborne earthquake of 2007. *Bnzsee*, *41*(4), 266–277. https://doi.org/10.5459/bnzsee.41.4.266-277

Gao, D., & Kao, H. (2020). Optimization of the match-filtering method for robust repeating earthquake detection: The multisegment cross-correlation approach. *Journal of Geophysical Research: Solid Earth*, *125*(7), e2020JB019714. https://doi.org/10.1029/2020jb019714

Gardonio, B., Marsan, D., Socquet, A., Bouchon, M., Jara, J., Sun, Q., et al. (2018). Revisiting slow slip events occurrence in Boso Peninsula, Japan, combining GPS data and repeating earthquakes analysis. *Journal of Geophysical Research: Solid Earth*, *123*(2), 1502–1515. https://doi.org/10.1002/2017jb014469

Hatakeyama, N., Uchida, N., Matsuzawa, T., & Nakamura, W. (2017). Emergence and disappearance of interplate repeating earthquakes following the 2011 M9.0 Tohoku-oki earthquake: Slip behavior transition between seismic and aseismic depending on the loading rate. *Journal of Geophysical Research: Solid Earth*, *122*(7), 5160–5180. https://doi.org/10.1002/2016jb013914

Havskov, J., & Ottemoller, L. (1999). SEISAN earthquake analysis software. *Seismological Research Letters*, *70*(5), 532–534. https://doi.org/10.1785/gssrl.70.5.532

Heise, W., Caldwell, T. G., Bannister, S., Bertrand, E. A., Ogawa, Y., Bennie, S. L., & Ichihara, H. (2017). Mapping subduction interface coupling using magnetotellurics: Hikurangi margin, New Zealand. *Geophysical Research Letters*, *44*(18), 9261–9266. https://doi.org/10.1002/2017gl074641

Hunter, J. D. (2007). Matplotlib: A 2D graphics environment. *Computing in Science & Engineering*, *9*(3), 90–95. https://doi.org/10.1109/mcse.2007.55

Igarashi, T., Matsuzawa, T., & Hasegawa, A. (2003). Repeating earthquakes and interplate aseismic slip in the northeastern Japan subduction zone. *Journal of Geophysical Research: Solid Earth*, *108*(B5), 1–8. https://doi.org/10.1029/2002jb001920

Jacobs, K., Savage, M., & Smith, E. (2016). Quantifying seismicity associated with slow slip events in the Hikurangi margin, New Zealand. *New Zealand Journal of Geology and Geophysics*, *59*(1), 58–69. https://doi.org/10.1080/00288306.2015.1127827

Johnson, L. R. (2010). An earthquake model with interacting asperities. *Geophysical Journal International*, *182*(3), 1339–1373. https://doi.org/10.1111/j.1365-246x.2010.04680.x

Kato, A., Obara, K., Igarashi, T., Tsuruoka, H., Nakagawa, S., & Hirata, N. (2012). Propagation of slow slip leading up to the 2011 Mw 9.0 Tohoku-Oki earthquake. *Science*, *335*(6069), 705–708. https://doi.org/10.1126/science.1215141

Koulali, A., McClusky, S., Wallace, L., Allgeyer, S., Tregoning, P., D'Anastasio, E., & Benavente, R. (2017). Slow slip events and the 2016 Te AraroaMw7.1 earthquake interaction: Northern Hikurangi subduction, New Zealand. *Geophysical Research Letters*, *44*(16), 8336–8344. https://doi.org/10.1002/2017gl074776

Krischer, L., Megies, T., Barsch, R., Beyreuther, M., Lecocq, T., Caudron, C., & Wassermann, J. (2015). ObsPy: A bridge for seismology into the scientific Python ecosystem. *Comput. Sci. Disc.*, *8*(1), 014003. https://doi.org/10.1088/1749-4699/8/1/014003

Langridge, R., Ries, W., Litchfield, N., Villamor, P., Van Dissen, R., Barrell, D., et al. (2016). The new zealand active faults database. *New Zealand Journal of Geology and Geophysics*, *59*(1), 86–96. https://doi.org/10.1080/00288306.2015.1112818

Lengliné, O., & Marsan, D. (2009). Inferring the coseismic and postseismic stress changes caused by the 2004 Mw6 Parkfield earthquake from variations of recurrence times of microearthquakes. *Journal of Geophysical Research: Solid Earth*, *114*(B10), 1–19. https://doi.org/10.1029/2008jb006118

Li, C., Peng, Z., Yao, D., Guo, H., Zhan, Z., & Zhang, H. (2018). Abundant aftershock sequence of the 2015 Mw7.5 Hindu Kush intermediate-depth earthquake. *Geophysical Journal International*, *213*(2), 1121–1134. https://doi.org/10.1093/gji/ggy016

Litchfield, N. J., Clark, K. J., Cochran, U. A., Palmer, A. S., Mountjoy, J., Mueller, C., et al. (2020). Marine terraces reveal complex near-shore upper-plate faulting in the northern Hikurangi margin, New Zealand. *Bulletin of the Seismological Society of America*, *110*(2), 825–849. https://doi.org/10.1785/0120190208

Lomax, A., Virieux, J., Volant, P., & Berge-Thierry, C. (2000). Probabilistic earthquake location in 3D and layered models. In *Advances in seismic event location* (pp. 101–134). Springer. https://doi.org/10.1007/978-94-015-9536-0_5

Lui, S. K. Y., & Lapusta, N. (2016). Repeating microearthquake sequences interact predominantly through postseismic slip. *Nature Communications*, *7*, 13020. https://doi.org/10.1038/ncomms13020

Marone, C., Vidale, J. E., & Ellsworth, W. L. (1995). Fault healing inferred from time dependent variations in source properties of repeating earthquakes. *Geophysical Research Letters*, *22*(22), 3095–3098. https://doi.org/10.1029/95gl03076

Materna, K., Taira, T. a., & Bürgmann, R. (2018). Aseismic transform fault slip at the mendocino triple junction from characteristically repeating earthquakes. *Geophysical Research Letters*, *45*(2), 699–707. https://doi.org/10.1002/2017gl075899

Mavrommatis, A. P., Segall, P., Uchida, N., & Johnson, K. M. (2015). Long-term acceleration of aseismic slip preceding the M w 9 Tohoku-oki earthquake: Constraints from repeating earthquakes. *Geophysical Research Letters*, *42*(22), 9717–9725. https://doi.org/10.1002/2015gl066069

Mesimeri, M., & Karakostas, V. (2018). Repeating earthquakes in western corinth gulf (greece): Implications for aseismic slip near locked faults. *Geophysical Journal International*, *215*(1), 659–676. https://doi.org/10.1093/gji/ggy301

Mountjoy, J. J., & Barnes, P. M. (2011). Active upper plate thrust faulting in regions of low plate interface coupling, repeated slow slip events, and coastal uplift: Example from the Hikurangi margin, New Zealand. *Geochemistry, Geophysics, Geosystems*, *12*(1). https://doi.org/10.1029/2010gc003326

Nadeau, R. M., Antolik, M., Johnson, P. A., Foxall, W., & McEvilly, T. V. (1994). Seismological studies at Parkfield III: Microearthquake clusters in the study of fault-zone dynamics. *Bulletin of the Seismological Society of America*, *84*(2), 247–263.

Nadeau, R. M., Foxall, W., & McEvilly, T. V. (1995). Clustering and periodic recurrence of microearthquakes on the San Andreas fault at Parkfield, California. *Science*, *267*(5197), 503–507. https://doi.org/10.1126/science.267.5197.503

Nadeau, R. M., & Johnson, L. R. (1998). Seismological studies at Parkfield VI: Moment release rates and estimates of source parameters for small repeating earthquakes. *Bulletin of the Seismological Society of America*, *88*(3), 790–814.

Nadeau, R. M., & McEvilly, T. V. (1999). Fault slip rates at depth from recurrence intervals of repeating microearthquakes. *Science*, *285*(5428), 718–721. https://doi.org/10.1126/science.285.5428.718

Naoi, M., Nakatani, M., Igarashi, T., Otsuki, K., Yabe, Y., Kgarume, T., et al. (2015). Unexpectedly frequent occurrence of very small repeating earthquakes ($-5.1 \leq Mw \leq -3.6$) in a South African gold mine: Implications for monitoring intraplate faults. *Journal of Geophysical Research: Solid Earth*, *120*(12), 8478–8493. https://doi.org/10.1002/2015jb012447

Nicol, A., & Wallace, L. M. (2007). Temporal stability of deformation rates: Comparison of geological and geodetic observations, Hikurangi subduction margin, New Zealand. *Earth and Planetary Science Letters*, *258*(3–4), 397–413. https://doi.org/10.1016/j.epsl.2007.03.039. https://doi.org/10.1016/j.epsl.2007.03.039

Nomura, S., Ogata, Y., Uchida, N., & Matsu'ura, M. (2017). Spatiotemporal variations of interplate slip rates in northeast Japan inverted from recurrence intervals of repeating earthquakes. *Geophysical Journal International*, *208*(1), 468–481. https://doi.org/10.1093/gji/ggw395

Passelègue, F. X., Almakari, M., Dublanchet, P., Barras, F., Fortin, J., & Violay, M. (2020). Initial effective stress controls the nature of earthquakes. *Nature Communications*, *11*(1), 1–8. https://doi.org/10.1038/s41467-020-18937-0

Peng, Z., Vidale, J. E., Marone, C., & Rubin, A. (2005). Systematic variations in recurrence interval and moment of repeating aftershocks. *Geophysical Research Letters*, *32*(15), 1–4. https://doi.org/10.1029/2005gl022626

Reasenberg, P. A. (1985). *FPFIT, FPPLOT, and FPPAGE: Fortran computer programs for calculating and displaying earthquake fault-plane solutions*. US Geol. Surv. Open-File Rep. 85-739.

Schaff, D. P., & Richards, P. G. (2004). Repeating seismic events in China. *Science*, *303*(5661), 1176–1178. https://doi.org/10.1126/science.1093422

Schaff, D. P., & Richards, P. G. (2011). On finding and using repeating seismic events in and near China. *Journal of Geophysical Research: Solid Earth*, *116*(B3), 1–20. https://doi.org/10.1029/2010jb007895

Schaff, D. P., & Richards, P. G. (2014). Improvements in magnitude precision, using the statistics of relative amplitudes measured by cross correlation. *Geophysical Journal International*, *197*(1), 335–350. https://doi.org/10.1093/gji/ggt433

Senobari, N. S., & Funning, G. J. (2019). Widespread fault creep in the northern San Francisco Bay Area revealed by multistation cluster detection of repeating earthquakes. *Geophysical Research Letters*, *46*(12), 6425–6434. https://doi.org/10.1029/2019GL082766

Shaddox, H. R., & Schwartz, S. Y. (2019). Subducted seamount diverts shallow slow slip to the forearc of the northern Hikurangi subduction zone, New Zealand. *Geology*, *47*(5), 415–418. https://doi.org/10.1130/g45810.1

Thomas, A. M., Beroza, G. C., & Shelly, D. R. (2016). Constraints on the source parameters of low-frequency earthquakes on the San Andreas Fault. *Geophysical Research Letters*, *43*(4), 1464–1471. https://doi.org/10.1002/2015gl067173

Todd, E. K., & Schwartz, S. Y. (2016). Tectonic tremor along the northern Hikurangi margin, New Zealand, between 2010 and 2015. *Journal of Geophysical Research: Solid Earth*, *121*(12), 8706–8719. https://doi.org/10.1002/2016jb013480

Todd, E. K., Schwartz, S. Y., Mochizuki, K., Wallace, L. M., Sheehan, A. F., Webb, S. C., et al. (2018). Earthquakes and tremor linked to seamount subduction during shallow slow slip at the Hikurangi margin, New Zealand. *Journal of Geophysical Research: Solid Earth*, *123*(8), 6769–6783. https://doi.org/10.1029/2018JB016136

Trugman, D. T., & Shearer, P. M. (2017). GrowClust: A hierarchical clustering algorithm for relative earthquake relocation, with application to the Spanish Springs and Sheldon, Nevada, earthquake sequences. *Seismological Research Letters*, *88*(2A), 379–391. https://doi.org/10.1785/0220160188

Uchida, N. (2019). Detection of repeating earthquakes and their application in characterizing slow fault slip. *Progress in Earth and Planetary Science*, *6*(1), 40–42. https://doi.org/10.1186/s40645-019-0284-z

Uchida, N., & Bürgmann, R. (2019). Repeating earthquakes. *Annual Review of Earth and Planetary Sciences*, *47*, 305–332. https://doi.org/10.1146/annurev-earth-053018-060119

Uchida, N., Hasegawa, A., Matsuzawa, T., & Igarashi, T. (2004). Pre-and post-seismic slow slip on the plate boundary off Sanriku, NE Japan associated with three interplate earthquakes as estimated from small repeating earthquake data. *Tectonophysics*, *385*(1–4), 1–15. https://doi.org/10.1016/j.tecto.2004.04.015

Uchida, N., Iinuma, T., Nadeau, R. M., Bürgmann, R., & Hino, R. (2016). Periodic slow slip triggers megathrust zone earthquakes in northeastern Japan. *Science*, *351*(6272), 488–492. https://doi.org/10.1126/science.aad3108

Uchida, N., & Matsuzawa, T. (2013). Pre- and postseismic slow slip surrounding the 2011 Tohoku-oki earthquake rupture. *Earth and Planetary Science Letters*, *374*, 81–91. https://doi.org/10.1016/j.epsl.2013.05.021

Uchida, N., Matsuzawa, T., Hasegawa, A., & Igarashi, T. (2003). Interplate quasi-static slip off Sanriku, NE Japan, estimated from repeating earthquakes. *Geophysical Research Letters*, *30*(15), 1–4. https://doi.org/10.1029/2003gl017452

Uchida, N., Matsuzawa, T., Hirahara, S., & Hasegawa, A. (2006). Small repeating earthquakes and interplate creep around the 2005 Miyagi-oki earthquake ($M = 7.2$). *Earth, Planets and Space*, *58*(12), 1577–1580. https://doi.org/10.1186/bf03352664

Virtanen, P., Gommers, R., Oliphant, T. E., Haberland, M., Reddy, T., & Cournapeau, D., et al.; SciPy 1.0 Contributors (2020). SciPy 1.0: Fundamental algorithms for scientific computing in Python. *Nature Methods*, *17*, 261–272. https://doi.org/10.1038/s41592-019-0686-2

Wallace, L. M. (2020). Slow slip events in New Zealand. *Annual Review of Earth and Planetary Sciences*, *48*, 1–8. https://doi.org/10.1146/annurev-earth-071719-055104

Wallace, L. M., & Beavan, J. (2010). Diverse slow slip behavior at the Hikurangi subduction margin, New Zealand. *Journal of Geophysical Research*, *115*(B12), 1–20. https://doi.org/10.1029/2010jb007717

Wallace, L. M., Beavan, J., Bannister, S., & Williams, C. (2012). Simultaneous long-term and short-term slow slip events at the Hikurangi subduction margin, New Zealand: Implications for processes that control slow slip event occurrence, duration, and migration. *Journal of Geophysical Research: Solid Earth*, *117*(B11), 1–18. https://doi.org/10.1029/2012jb009489

Wallace, L. M., Beavan, J., McCaffrey, R., & Darby, D. (2004). Subduction zone coupling and tectonic block rotations in the North Island, New Zealand. *Journal of Geophysical Research: Solid Earth*, *109*(B12), 1–21. https://doi.org/10.1029/2004jb003241

Wallace, L. M., & Eberhart-Phillips, D. (2013). Newly observed, deep slow slip events at the central Hikurangi margin, New Zealand: Implications for downdip variability of slow slip and tremor, and relationship to seismic structure. *Geophysical Research Letters*, *40*(20), 5393–5398. https://doi.org/10.1002/2013gl057682

Wallace, L. M., Hreinsdóttir, S., Ellis, S., Hamling, I., D'Anastasio, E., & Denys, P. (2018). Triggered slow slip and afterslip on the southern Hikurangi subduction zone following the Kaikōura earthquake. *Geophysical Research Letters*, *45*(10), 4710–4718. https://doi.org/10.1002/2018gl077385

Wallace, L. M., Kaneko, Y., Hreinsdóttir, S., Hamling, I., Peng, Z., Bartlow, N., et al. (2017). Large-scale dynamic triggering of shallow slow slip enhanced by overlying sedimentary wedge. *Nature Geoscience*, *10*(10), 765–770. https://doi.org/10.1038/ngeo3021

Wallace, L. M., Reyners, M., Cochran, U., Bannister, S., Barnes, P. M., Berryman, K., et al. (2009). Characterizing the seismogenic zone of a major plate boundary subduction thrust: Hikurangi margin, New Zealand. *Geochemistry, Geophysics, Geosystems*, *10*(10), 1–32. https://doi.org/10.1029/2009gc002610

Wallace, L. M., Webb, S. C., Ito, Y., Mochizuki, K., Hino, R., Henrys, S., et al. (2016). Slow slip near the trench at the Hikurangi subduction zone, New Zealand. *Science*, *352*(6286), 701–704. https://doi.org/10.1126/science.aaf2349

Warren-Smith, E., Fry, B., Kaneko, Y., & Chamberlain, C. J. (2018). Foreshocks and delayed triggering of the 2016 MW7.1 Te Araroa earthquake and dynamic reinvigoration of its aftershock sequence by the MW7.8 Kaikōura earthquake, New Zealand. *Earth and Planetary Science Letters*, *482*, 265–276. https://doi.org/10.1016/j.epsl.2017.11.020

Warren-Smith, E., Fry, B., Wallace, L., Chon, E., Henrys, S., Sheehan, A., et al. (2019). Episodic stress and fluid pressure cycling in subducting oceanic crust during slow slip. *Nature Geoscience*, *12*(6), 475–481. https://doi.org/10.1038/s41561-019-0367-x

Wessel, P., Luis, J. F., Uieda, L., Scharroo, R., Wobbe, F., Smith, W. H. F., & Tian, D. (2019). The generic mapping tools version 6. *Geochemistry, Geophysics, Geosystems*, *20*(11), 5556–5564. https://doi.org/10.1029/2019gc008515

Wiemer, S., & Wyss, M. (2000). Minimum magnitude of completeness in earthquake catalogs: Examples from Alaska, the western United States, and Japan. *Bulletin of the Seismological Society of America*, *90*(4), 859–869. https://doi.org/10.1785/0119990114

Williams, C. A., Eberhart-Phillips, D., Bannister, S., Barker, D. H. N., Henrys, S., Reyners, M., & Sutherland, R. (2013). Revised interface geometry for the Hikurangi subduction zone, New Zealand. *Seismological Research Letters*, *84*(6), 1066–1073. https://doi.org/10.1785/0220130035

Williams, J. R., Hawthorne, J. C., & Lengliné, O. (2019). The long recurrence intervals of small repeating earthquakes may be due to the slow slip rates of small fault strands. *Geophysical Research Letters*, *46*(22), 12823–12832. https://doi.org/10.1029/2019gl084778

Wu, C., Gomberg, J., Ben-Naim, E., & Johnson, P. (2014). Triggering of repeating earthquakes in central California. *Geophysical Research Letters*, *41*(5), 1499–1505. https://doi.org/10.1002/2013gl059051

Yamashita, Y., Shimizu, H., & Goto, K. (2012). Small repeating earthquake activity, interplate quasi-static slip, and interplate coupling in the Hyuga-nada, southwestern Japan subduction zone. *Geophysical Research Letters*, *39*(8), 1–5. https://doi.org/10.1029/2012gl051476

Yao, D., Walter, J. I., Meng, X., Hobbs, T. E., Peng, Z., Newman, A. V., et al. (2017). Detailed spatiotemporal evolution of microseismicity and repeating earthquakes following the 2012 Mw 7.6 Nicoya earthquake. *Journal of Geophysical Research: Solid Earth*, *122*(1), 524–542. https://doi.org/10.1002/2016jb013632

Yarce, J., Sheehan, A. F., Nakai, J. S., Schwartz, S. Y., Mochizuki, K., Savage, M. K., et al. (2019). Seismicity at the northern Hikurangi margin, New Zealand, and investigation of the potential spatial and temporal relationships with a shallow slow slip event. *Journal of Geophysical Research: Solid Earth*, *124*(1), 4751–4766. https://doi.org/10.1029/2018jb017211

Yu, W. c. (2013). Shallow-focus repeating earthquakes in the Tonga-Kermadec-Vanuatu subduction zones. *Bulletin of the Seismological Society of America*, *103*(1), 463–486. https://doi.org/10.1785/0120120123

Zhang, J., Richards, P. G., & Schaff, D. P. (2008). Wide-scale detection of earthquake waveform doublets and further evidence for inner core super-rotation. *Geophysical Journal International*, *174*(3), 993–1006. https://doi.org/10.1111/j.1365-246x.2008.03856.x